

Constraining models of initial state with v_2 and v_3 data from LHC and RHIC

Ekaterina Retinskaya^{a,*}, Matthew Luzum^{b,c}, Jean-Yves Ollitrault^d

^aCEA, IPhT, Institut de physique théorique de Saclay, F-91191 Gif-sur-Yvette, France

^bMcGill University, 3600 University Street, Montreal QC H3A 2T8, Canada

^cLawrence Berkeley National Laboratory, Berkeley, CA 94720, USA

^dCNRS, URA2306, IPhT, Institut de physique théorique de Saclay, F-91191 Gif-sur-Yvette, France

Abstract

We present a combined analysis of elliptic and triangular flow data from LHC and RHIC using viscous relativistic hydrodynamics. Elliptic flow v_2 in hydrodynamics is proportional to the participant eccentricity ε_2 and triangular flow is proportional to the participant triangularity ε_3 , which means $v_n = C_n \varepsilon_n$, where C_n is the linear response coefficient in harmonic n . Experimental data for v_2 and v_3 combined with hydrodynamic calculations of C_n thus provide us with the rms values of initial anisotropies ε_2 and ε_3 . By varying free parameters in the hydro calculation (in particular the shear viscosity), we obtain an allowed band in the (rms ε_2 , rms ε_3) plane. Comparison with Monte-Carlo models of the initial state allows us to exclude several of these models. We illustrate that the effect of changing the granularity of the initial state is similar to changing the medium properties, making these effects difficult to disentangle.

1. Introduction

One of the most important topics of study in heavy-ion collisions is the observation of particle momentum anisotropy in directions transverse to the beam [1], which can provide the evidence for the formation of some strongly interacting medium, which thermalizes and expands as a liquid, which we call the quark-gluon plasma (QGP). The corresponding experimental observables are the flow coefficients v_1 , v_2 , v_3 etc. In these proceedings we will concentrate on v_2 and v_3 (elliptic [3, 4] and triangular) flow coefficients. While elliptic flow, v_2 , is a response of the system to an initial distribution with the form of ellipse in the transverse plane [5], the triangular flow, v_3 , is understood as the response of triangular deformation, which is caused by fluctuations of initial geometry [6].

In spite of the fact that v_2 and v_3 are the most studied harmonics of anisotropic flow, there are still a number of open questions. Different models of initial states give different values when trying to extract transport coefficients from data. For instance by tuning η/s (viscosity over entropy [7]) one can match the experimental data with one model or another [8]. And it was found out that although one could fit both v_2 and v_3 data separately by tuning η/s with hydro

*Corresponding author

Email addresses: ekaterina.retinskaya@cea.fr (Ekaterina Retinskaya), MWLuzum@lbl.gov (Matthew Luzum), jean-yves.ollitrault@cea.fr (Jean-Yves Ollitrault)

Preprint submitted to Nuclear Physics A

July 16, 2018

calculation, some of the models of initial state were unable to fit simultaneously v_2 and v_3 [9, 10]. This hints, that by combining v_2 and v_3 data we can constrain models of initial state even though the viscosity is unknown.

2. Monte Carlo models of initial state

By initial conditions, we mean the initial energy-density profile at thermalization time t_0 [31]. This profile is not smooth and has fluctuations from wave-functions of incoming nuclei. The magnitude of these fluctuations is still to a large extent unconstrained from data. Another open question pertaining to initial state is how elongated is the ellipse of the overlap area in non-central collisions. We will address these issues and test different Monte Carlo models of initial state. We are testing two types of models: Glauber-type models and QCD-inspired models. The Monte Carlo Glauber model is the oldest and the most classic one [13]. We use the PHOBOS Monte Carlo [14]. In this model positions of nucleons within a nuclei are sampled through Monte Carlo. These nucleons move on straight lines and interact if their distance is less then $\sqrt{\sigma_{NN}}/\pi$. Typically one then models each nucleon as a Gaussian source, so that the final energy-density is equal to a sum of Gaussians.

Among the QCD-inspired models we are going to test 4 of them: the oldest QCD model which we call MC-KLN [15, 16], which is using k_T factorization and taking into account fluctuations of the positions of the nucleons. The second model MCrcBK [18] is an improved MC-KLN model with additional KNO fluctuations in order to match multiplicity distribution in pp collisions. The third one is DIPSY [17], a QCD model which takes into account the multiple gluon cascade. And the last one is the IP Glasma model [19], which doesn't assume k_T factorization and includes non-linearities and fluctuations of color charges within a nucleon.

3. Hydro evolution

In spite of the fact that collaborations have published data for integrated v_n [12] for $n=1, 2, \dots, 6$ [20], here we only use elliptic and triangular flow. The main reason is that these two Fourier coefficients are determined by simple linear response to the initial state [21]. That means: $v_2 \propto \varepsilon_2$ [22], where ε_2 is called participant ellipticity [23] and $v_3 \propto \varepsilon_3$ [24], ε_3 is called participant triangularity [6]. The participant eccentricity ε_n for a single event is defined as [2, 25]:

$$\varepsilon_n = \frac{|\{r^n e^{in\phi}\}|}{\{r^n\}}, \quad (1)$$

where $\{\dots\}$ denotes an average value over the initial energy density (it can also be entropy density profile though) after recentering the coordinate system $\{re^{i\phi}\} = 0$.

Assuming linear response to the initial anisotropy, the anisotropic flow in an event is $v_n = C_n \varepsilon_n$. The response coefficient C_n is the same for all events in a centrality bin, but ε_n fluctuates, so that initial-state fluctuations result in event-by-event flow fluctuations. Experiments measure the rms value of v_n over a centrality bin, thus the experimentally measured flow v_n is proportional to the rms value of ε_n . We can therefore write:

$$\sqrt{\langle \varepsilon_n^2 \rangle} = \frac{\sqrt{\langle (v_n)^2 \rangle}}{C_n}, \quad (2)$$

where $\sqrt{\langle(v_n)^2\rangle}$ is the measured root mean square value of integrated flow and $\langle...\rangle$ represents an average over collision events. The response coefficient C_n is calculated in hydrodynamics as $C_n = (v_n/\varepsilon_n)_{hydro}$, so that we are able to extract the root mean square values of ε_2 and ε_3 . We take experimental data of integrated flow from the ALICE and PHENIX collaborations [10, 11].

4. Uncertainties in hydro response

The standard hydro modeling [26] procedure consist of 3 main steps:

- 1) initial conditions
- 2) evolve these initial conditions through relativistic hydro evolution
- 3) convert the liquid into hadrons at freeze-out temperature.

Each of these steps obviously has its uncertainties [27]. The main uncertainty in the hydro evolution is the value of the shear viscosity of the strongly-interacting quark-gluon plasma. This value is not constrained well in theory and experiment[35, 36], so we vary η/s as a parameter from 0 to 0.24 in steps of 0.04. The value of the shear viscosity has a remarkable influence on the values of integrated flow: the flow decreases with increasing viscosity. Another big source of uncertainty is coming from initial conditions. Our hydro calculations are 2+1D viscous hydrodynamic, which uses as input initial condition the transverse energy density profile from an optical Glauber model. This profile is smooth and already has an ellipticity, so automatically gives us elliptic flow values. If we want to obtain the values of ε_3 or v_3 , with this profile we get 0 for both of them, so in order to calculate C_3 we deform the third harmonic in the profile in the following way [9] :

$$\epsilon(r, \phi) \rightarrow (r \sqrt{1 + \varepsilon'_n \cos(n(\phi - \psi_n))}, \phi) \quad (3)$$

where ε'_n is magnitude of the deformation, and ψ_n is the orientation of the deformation.

In order to estimate the uncertainty on the value of C_n from the initial profile, we use two definitions of ε_n : with energy density weighting and entropy density weighting.

Another free parameter is the thermalization time t_0 [31, 32] which is not known. We vary it from 0.5 fm/c to 1fm/c. While we vary the thermalization time we tune the starting temperature T_{start} and the freeze-out temperature T_{fr} so as to match the p_t spectrum [29, 30].

In the hadronic part we also have some uncertainty, which is coming from the freezeout viscous correction, the momentum dependence of which is unknown[37, 38, 39], so we test 2 possible ansatzs: linear $\propto p$ [40] and quadratic $\propto p^2$ [37]. We use the same code as in Ref.[38] and we take into account resonance decays after hadronization.

After taking into account all types of uncertainties we can calculate ε_2 and ε_3 using Eq. (2). The resulting values are shown in the Fig. 1 for the most central collisions at the LHC.

Each point in this figure corresponds to one hydro calculation with one set of parameters. We have 6 types of symbols, corresponding different sets of parameters: thermalization time t_0 , the type of ansatz and the type of ε_n weighting. These symbols are composing 6 lines with viscosity η/s changing. Each line has 7 points, corresponding to $\eta/s = 0, 0.04, 0.08, 0.12, 0.16, 0.2, 0.24$ (from left to right). The first line, composed of blue circles, uses as parameters the thermalization time 1fm/c and the linear ansatz. The line with purple squares uses thermalization time 1fm/c and quadratic ansatz. We see the line almost doesn't change, except for high viscosity, which makes values of ε_2 slightly smaller. The line composed of yellow diamonds corresponds to thermalization time 0.5 fm/c and quadratic ansatz. We see that ε_2 and ε_3 are both decreasing. The explanation is that since we start the hydro evolution earlier, we produce more flow, and from

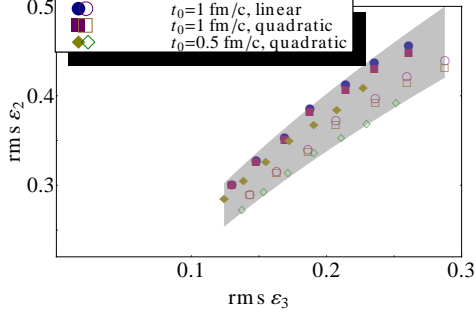


Figure 1: (Color online) R.m.s. values of $\epsilon_2(\epsilon_3)$ from hydro simulations + ALICE data for 20-30% centrality range. Purple squares correspond to $t_{init} = 1 \text{ fm/c}$ with quadratic freezeout. Blue circles correspond to $t_{init} = 1 \text{ fm/c}$ with linear freezeout. Yellow diamonds correspond to $t_{init} = 0.5 \text{ fm/c}$ with quadratic freezeout. Open symbols mean entropy-density profile used. The shaded band is an allowed band encompassing uncertainty in the extracted values.

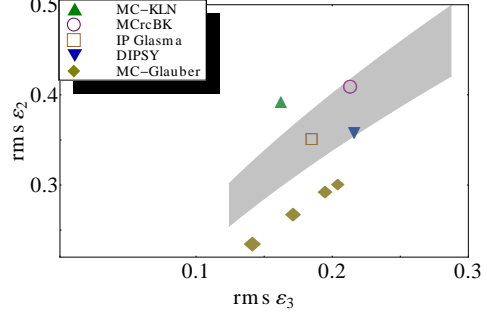


Figure 2: (Color online) The shaded band is the same as in Fig.1 and represents allowed values. Symbols are predictions from various models of initial state. The MC-Glauber model is shown for different values of the width of gaussian $\sigma=0 \text{ fm}$, 0.4 fm , 0.8 fm and 1.2 fm , which are distinguished by different symbol sizes, showing that changing the smearing parameter has the same effect as changing viscosity.

the ratio (2) obviously if we produce more flow, we will have smaller values of ϵ_2 and ϵ_3 . Lines composed of open symbols have the same parameters, except that entropy-density weighting is used. Now we create a shaded band, such that all these points are inside this band. This band defines the allowed range. The important fact here is that even with all uncertainties taken into account, we obtain a narrow band, which eventually allows us to constrain models. These lines are noticed to be well fitted by the law $\sqrt{\langle \epsilon_2^2 \rangle} / \left(\sqrt{\langle \epsilon_3^2 \rangle} \right)^k = C$, where $k=0.6$ for LHC and $k=0.5$ for RHIC and C is fixed. By computing the maximum and minimum values of C allowed by hydrodynamics, we determine the range of allowed values for C .

By computing the values of C in various Monte Carlo models, one can check if the values predicted by models are inside the allowed region, as shown in Fig. 3. In this way the formula can be used easily by any group who has an MC model of initial states in order to see if their model is compatible with experimental data.

5. Results

We calculate the allowed region in the $(\text{rms } \epsilon_2, \text{rms } \epsilon_3)$ plane for different centralities for LHC and RHIC, which we represent as a shaded band. After this we test the models, introduced in Section 2.

In Fig. 2 we display as an example the 20-30% centrality range. The MC-Glauber model is shown for different values of the width of gaussian $\sigma=0 \text{ fm}$, 0.4 fm , 0.8 fm and 1.2 fm , which are distinguished by different symbol sizes. By changing this parameter the result moves parallel to the band, which has the same effect as changing the viscosity, so that compatibility with data cannot be improved by adjusting the unknown source size.

Our main results are presented in Fig. 3. It displays the rms values of $\sqrt{\langle \epsilon_2^2 \rangle} / \left(\sqrt{\langle \epsilon_3^2 \rangle} \right)^k$ versus centrality, where shaded bands are allowed values and symbols are predictions from different

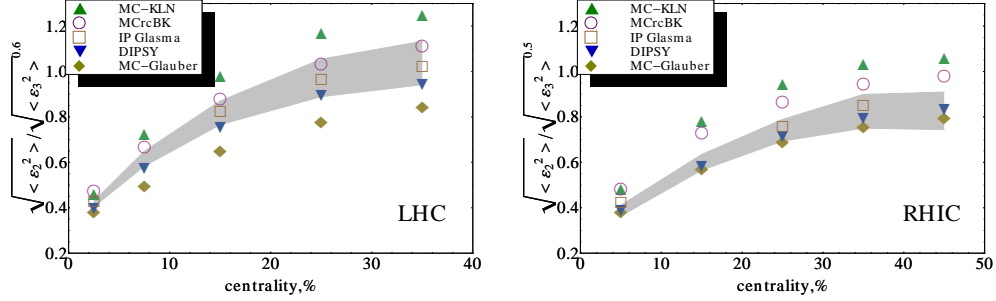


Figure 3: (Color online) Ratio of eccentricity moments $\sqrt{\langle \varepsilon_2^2 \rangle} / \left(\sqrt{\langle \varepsilon_3^2 \rangle} \right)^k$ versus centrality. Shaded bands are allowed by experiment values, combined with hydrodynamic calculations, for LHC and RHIC. Symbols are predictions from various models of initial state.

models. We can see that one can exclude MC-Glauber (as was also noticed for 20-30% centrality) and MC-KLN models for LHC energies. It seems MC Glauber works better for lower energies, and MC-KLN doesn't have enough fluctuations. For RHIC energies MC-KLN can also be excluded, along with the MCrcBK model, which seems to work better at LHC energies.

From the Fig.2 in our paper [41] we've seen that rms ε_2 and ε_3 values predicted by MC models both increase with centrality, but we noticed that ε_2 values are increasing faster than ε_3 , which can be explained by the fact, that v_2 is growing faster with centrality than v_3 : v_2 grows due to geometry, and v_3 due to the fact that fluctuations have more influence with increasing centrality, but this effect is weaker. By looking at the ε_3 values of MC models we can see which of the models have more fluctuations, for example by comparing MC-KLN and MCrcBK, obviously, the second has more fluctuations, as the result it has bigger value of ε_3 . The same about DIPSY which seems to have big value of fluctuations.

Conclusions

We have extracted ellipticity ε_2 and triangularity ε_3 , using experimental data and hydro calculations with different sources of uncertainties and created a narrow allowed region on the (rms ε_3 , rms ε_2) plane. We have shown that we are able to constrain models of initial state. It was shown that we can exclude MC-Glauber and MC-KLN models for LHC and MC-KLN and MCrcBK models for RHIC. We have illustrated for the MC Glauber model that changing the granularity of the initial condition model has the same effect as changing viscosity, so the effects are difficult to disentangle.

More details about this study can be found in our recently published paper [41].

References

- [1] S. A. Voloshin, A. M. Poskanzer and R. Snellings, arXiv:0809.2949 [nucl-ex].
- [2] D. Teaney and L. Yan, Phys. Rev. C **83**, 064904 (2011) [arXiv:1010.1876 [nucl-th]].
- [3] K. H. Ackermann *et al.* [STAR Collaboration], Phys. Rev. Lett. **86**, 402 (2001) [nucl-ex/0009011].
- [4] K. Aamodt *et al.* [ALICE Collaboration], Phys. Rev. Lett. **105**, 252302 (2010) [arXiv:1011.3914 [nucl-ex]].
- [5] J. -Y. Ollitrault, Phys. Rev. D **46**, 229 (1992).

- [6] B. Alver and G. Roland, Phys. Rev. C **81**, 054905 (2010) [Erratum-ibid. C **82**, 039903 (2010)] [arXiv:1003.0194 [nucl-th]].
- [7] P. Kovtun, D. T. Son and A. O. Starinets, Phys. Rev. Lett. **94**, 111601 (2005) [hep-th/0405231].
- [8] M. Luzum and P. Romatschke, Phys. Rev. C **78**, 034915 (2008) [Erratum-ibid. C **79**, 039903 (2009)] [arXiv:0804.4015 [nucl-th]].
- [9] B. H. Alver, C. Gombeaud, M. Luzum and J. -Y. Ollitrault, Phys. Rev. C **82**, 034913 (2010) [arXiv:1007.5469 [nucl-th]].
- [10] A. Adare *et al.* [PHENIX Collaboration], Phys. Rev. Lett. **107**, 252301 (2011) [arXiv:1105.3928 [nucl-ex]].
- [11] K. Aamodt *et al.* [ALICE Collaboration], Phys. Rev. Lett. **107**, 032301 (2011) [arXiv:1105.3865 [nucl-ex]].
- [12] N. Borghini, P. M. Dinh and J. -Y. Ollitrault, Phys. Rev. C **63**, 054906 (2001) [nucl-th/0007063].
- [13] M. L. Miller, K. Reygers, S. J. Sanders and P. Steinberg, Ann. Rev. Nucl. Part. Sci. **57**, 205 (2007) [nucl-ex/0701025].
- [14] B. Alver, M. Baker, C. Loizides and P. Steinberg, arXiv:0805.4411 [nucl-ex].
- [15] H. -J. Drescher and Y. Nara, Phys. Rev. C **76**, 041903 (2007) [arXiv:0707.0249 [nucl-th]].
- [16] J. L. Albacete and A. Dumitru, arXiv:1011.5161 [hep-ph].
- [17] C. Flensburg, arXiv:1108.4862 [nucl-th].
- [18] A. Dumitru and Y. Nara, Phys. Rev. C **85**, 034907 (2012) [arXiv:1201.6382 [nucl-th]].
- [19] B. Schenke, P. Tribedy and R. Venugopalan, Phys. Rev. C **86**, 034908 (2012) [arXiv:1206.6805 [hep-ph]].
- [20] G. Aad *et al.* [ATLAS Collaboration], Phys. Rev. C **86**, 014907 (2012) [arXiv:1203.3087 [hep-ex]].
- [21] H. Niemi, G. S. Denicol, H. Holopainen and P. Huovinen, Phys. Rev. C **87**, 054901 (2013) [arXiv:1212.1008 [nucl-th]].
- [22] H. Holopainen, H. Niemi and K. J. Eskola, Phys. Rev. C **83**, 034901 (2011) [arXiv:1007.0368 [hep-ph]].
- [23] B. Alver *et al.* [PHOBOS Collaboration], Phys. Rev. Lett. **98**, 242302 (2007) [nucl-ex/0610037].
- [24] H. Petersen, G. -Y. Qin, S. A. Bass and B. Muller, Phys. Rev. C **82**, 041901 (2010) [arXiv:1008.0625 [nucl-th]].
- [25] R. S. Bhalerao, M. Luzum and J. -Y. Ollitrault, Phys. Rev. C **84**, 034910 (2011) [arXiv:1104.4740 [nucl-th]].
- [26] C. Gale, S. Jeon and B. Schenke, Int. J. Mod. Phys. A **28**, 1340011 (2013).
- [27] M. Luzum and J. -Y. Ollitrault, Nucl. Phys. A904-905 **2013**, 377c (2013) [arXiv:1210.6010 [nucl-th]].
- [28] R. A. Soltz, I. Garishvili, M. Cheng, B. Abelev, A. Glenn, J. Newby, L. A. Linden Levy and S. Pratt, Phys. Rev. C **87**, 044901 (2013) [arXiv:1208.0897 [nucl-th]].
- [29] L. Adamczyk *et al.* [STAR Collaboration], Phys. Rev. C **88**, 014904 (2013) [arXiv:1301.2187 [nucl-ex]].
- [30] M. Luzum and P. Romatschke, Phys. Rev. Lett. **103**, 262302 (2009) [arXiv:0901.4588 [nucl-th]].
- [31] F. Gelis and T. Epelbaum, arXiv:1307.2214 [hep-ph].
- [32] P. F. Kolb and U. W. Heinz, In *Hwa, R.C. (ed.) et al.: Quark gluon plasma* 634-714 [nucl-th/0305084].
- [33] W. Broniowski, M. Chojnacki, W. Florkowski and A. Kisiel, Phys. Rev. Lett. **101**, 022301 (2008) [arXiv:0801.4361 [nucl-th]].
- [34] S. Pratt, Phys. Rev. Lett. **102**, 232301 (2009) [arXiv:0811.3363 [nucl-th]].
- [35] H. B. Meyer, Phys. Rev. D **76**, 101701 (2007) [arXiv:0704.1801 [hep-lat]].
- [36] H. Song, Nucl. Phys. A904-905 **2013**, 114c (2013) [arXiv:1210.5778 [nucl-th]].
- [37] D. Teaney, Phys. Rev. C **68**, 034913 (2003) [nucl-th/0301099].
- [38] D. Teaney and L. Yan, arXiv:1304.3753 [nucl-th].
- [39] K. Dusling, G. D. Moore and D. Teaney, Phys. Rev. C **81**, 034907 (2010) [arXiv:0909.0754 [nucl-th]].
- [40] M. Luzum and J. -Y. Ollitrault, Phys. Rev. C **82**, 014906 (2010) [arXiv:1004.2023 [nucl-th]].
- [41] E. Retinskaya, M. Luzum and J. -Y. Ollitrault, Phys. Rev. C **89**, 014902 (2014) [arXiv:1311.5339 [nucl-th]].